**European Journal of Clinical Pharmacy**
**Print ISSN:** 2385-409X **Online ISSN**: 3105-0409
Website: https://farmclin.com/

*Original Research Article*

# FORMULATION, CHARACTERIZATION, AND IN VITRO EVALUATION OF URSOLIC ACID-LOADED SOLID LIPID NANOPARTICLES FOR ENHANCED CYTOTOXICITY AGAINST HUMAN CANCER CELL LINE

***Article History:***

**Name of Author:**
Anasuya Patil[1], Jyoti[2], Rekha Tarasingh Rajput[3], Preeti Garg[4], Ajesh Chauhan[5], Ratne Nandini[6], Reshma.H.Pakali[7], Pankaj Pradhan*[8]

***Affiliation:*** *[1]Department of Pharmaceutics, KLE College of Pharmacy, II Block Rajajinagar, Bengaluru, KLE Academy Higher Education and Research. Belgavi-590 010, Karnataka, India;*
*[2]Assistant Professor, Hindu College of Pharmacy Sonipat, Near Panchayat Bhawan, Gohana Road, Sonipat - 131001, Haryana,*
*[3]Associate Professor, Sharda School of Pharmacy, Agra and Assistant Dean (Research and Development Cell, Sharda University, Agra), Sharda University, Agra.*
*[4]Assistant Professor, Hindu College of Pharmacy Sonipa, Near Panchayat Bhawan, Gohana Road, Sonipat - 131001, Haryana;*
*[5]Assistant Professor, Hindu College of Pharmacy Sonipat, Near Panchayat Bhawan, Gohana Road, Sonipat - 131001, Haryana;*
*[6]Nagpur College of Pharmacy, Wanadongri, Hingna Road, Nagpur, 441110*
*[7]Assistant Professor, Danigond college of pharmacy Terdal,*
*[8]Professor, Swami Keshvanand Institute of Pharmacy, Jaipur, R-30, Shyam Vihar, Railway Station Road, Chomu, Jaipur, Rajasthan-303702;*

***Corresponding Author:***
Pankaj Pradhan

***Abstract***: Ursolic acid (UA), which is a natural anticancer compound, is limited by low solubility and bioavailability inhibiting its application in medicine. This paper designed and tested solid lipid nanoparticles (SLNs) as a superior delivery system to address these drawbacks. PLGA and nanoprecipitation were employed successfully to produce small (134-167 nm) and uniform PLGA-PEG nanoparticles that are negatively charged with the formation of encapsulation efficiency of up to 45 percent. The nanoparticles were found to have increased cytotoxicity over breast (MDA-MB-231, MCF-7) cancer cell lines. The fast internalization of nanoparticles was verified in cellular uptake studies that took not more than two hours. Moreover, the formulations had good short term stability. Such results suggest that UA-loaded nanoparticles represent an important solution to enhance the delivery and effectiveness of this insoluble antimalignant agent.

*Keywords*: Ursolic acid; Nanoparticles; Drug delivery; Cytotoxicity; Cancer; PLGA; Nanomedicine; Cellular uptake

 

How to Cite: A. Patil, Jyoti, R.T. Rajput, P. Garg, A. Chauhan, R. Nandini, R.H. Pakali, P. Pradhan*.FORMULATION, CHARACTERIZATION, AND IN VITRO EVALUATION OF URSOLIC ACID-LOADED SOLID LIPID NANOPARTICLES FOR ENHANCED CYTOTOXICITY AGAINST HUMAN CANCER CELL LINE." *European Journal of Clinical Pharmacy*. 2025;7(1):3170-3179.

***Received:*** 12-11-2025
***Revised:*** 26-11-2025
***Accepted:*** 09-12-2025
***Published:*** 23-12-2025



## INTRODUCTION

Cancer has been among the strongest health threats to the whole world with traditional chemotherapy being a form of first-line intervention. Nevertheless, chemotherapeutic agents often have serious limitations that compromise their clinical efficacy such as excessive systemic toxicity against normal tissues, multidrug resistance in malignant cells, low aqueous solubility of most potent drugs, and non-specific biodistribution and resulting low therapeutic indices.[1] Such difficulties demand the creation of new approaches that would allow the delivery of anticancer agents to malignant sites in a more selective and efficient way with the least amount of adverse effects. In this regard, natural compounds have received a significant level of interest as targets of new chemotherapeutic and chemopreventive agents because of their variety in pharmacological activities and, in many cases, good safety profiles.[2] One of them, ursolic acid (UA), a pentacyclic triterpenoid, which is common in the peels of fruits and other medicinal herbs (e.g. Rosmarinus officinalis and Ocimum sanctum) has become promising. UA has the diverse pharmacological activities with potent anticancer effects achieved by inducing apoptosis, inhibiting cell proliferation, angiogenesis, and metastasis.[3][4][5] Its pathways are complex, entailing regulation of major signaling pathways, including PI3K/Akt, MAPK and NF-kB, and the activation of caspases and disruption of mitochondrial membrane potential. Although this is a good pharmacological profile, the inherent physicochemical characteristics of UA such as very low aqueous solubility, resulting in low oral bioavailability, coupled with rapid metabolism and systemic excretion, severely affect its clinical translation.[6][7] These drug kinetic shortcomings lead to inadequate concentrations of the drug to the tumor site that limits its therapeutic effects in vivo. In an effort to curb such daunting obstacles, drug delivery systems based on nanotechnology has been widely developed as a paradigm shift in the field of cancer. Nanotechnology has the unparalleled capability to physicochemically modify the pharmacokinetics and biodistribution of encapsulated drugs to offer solutions to solubility enhancement, sustained release, passive tumor targeting via enhanced permeability and retention (EPR) effect and potentially active tumor targeting by modifying surface ligands.[8][9] Among the various varieties of nanocarriers, such as liposomes, polymeric nanoparticles, and micelles, solid lipid nanoparticles (SLNs) have taken the center stage as an excellent colloidal carrier system of lipophilic molecule such as UA. SLNs are sub micron size particles formed of physiologically tolerated solid lipids which are solid at room and body temperature and are stabilized by surfactants.[11] They start combining the benefits of classical colloidal system, such as good biocompatibility and biodegradability of emulsions and the controlled release of polymeric nanoparticles, but at the same time, overcome some of the limitations of the system, e.g. residues of organic solvents and scale-up problems. In the case of lipophilic anticancer agents, SLNs have a high drug loading capacity, shielding against the breakdown of the encapsulating drug, capability to produce large volumes of systems through a high-pressure homogenization process, and the development of a long systemic residence.[12][13] Moreover, they can be lipidic and therefore improve cellular uptake, particularly in cancer cells and their small particle size (usually 50-300 nm) facilitates passive accumulation in tumor tissues because of the porous vasculature.[14]

A large body of preclinical research in a large range of human cancer cell lines (breast (MCF-7, MDA-MB-231), lung (A549), prostate (PC-3), colon (HCT-116), and cervical (HeLa) cancers) has demonstrated the anticancer potential of ursolic acid. The results of these studies show that UA has the capability of suppressing growth and causing programmed cell death.

Nevertheless, the established translational differences between these encouraging in vitro findings and in vivo effectiveness are already well understood, and it is mainly due to the aforementioned pharmacokinetic issues.[14][15] There have therefore been increased studies on developing UA in a number of nanocarrier systems to enhance its delivery. The published literature has covered UA encapsulation in liposomes, nanoemulsions, polymeric nanoparticles (e.g., PLGA) and cyclodextrin complexes where it was reported that the encapsulation improved the solubility, stability, and cytotoxicity of UA relative to free UA. All systems have their own advantages and disadvantages in terms of loading efficiency profile of release and the complexity of formulation. In this nanotecnological environment, SLNs offer certain promise because they have a distinctive matrix. Recent studies on the delivery of anticancer drugs using SLNs are well-prepared of a variety of synthetic and natural drugs, including paclitaxel, doxorubicin, and curcumin. These studies give a solid ground level justification and prove that SLNs have the capacity to increase cytotoxicity, induce apoptosis, overturn multidrug resistance, and elevate the therapeutic index of their payloads both in vitro and in vivo. Most commonly, the performance of such systems is tested by standardized models of in vitro cytotoxicity, which are essential to cancer nanomedicine as a first-line screening tool. Measures such as MTT, XTT and Alamar blue give quantitative analysis of cell viability and metabolic activity after treatment, which enables the calculation of half-maximal inhibitory concentration (IC50). Advanced in vitro models, including 3D spheroids and co culture models are being used more frequently to better model the tumor microenvironment. Such cytotoxicity assays are essential when comparing the potency of the formulated drug versus its free counterpart, the safety of blank carriers and understanding the mechanisms of action by complementary assays of apoptosis (Annexin V/PI), cell cycles of flow cytometry) and the generation of reactive oxygen species and depolarization of mitochondrial membranes. Although the data on UA is promising and the role of SLNs in oncology is proven to be essential, a closer examination of the extant literature will indicate that there are research gaps that are identified and the current study will attempt to fill them. Although past studies have discussed UA in different nanoformulations, a systematic and detailed approach to the formulation, optimization and characterization of UA-loaded SLNs specifically developed to take the inherent benefits of the solid lipid matrix are not fully reported. A lot of research could be conducted on a single factor, e.g. formulation or in vitro cytotoxicity, [16] but a unifying study should be conducted between a detailed physicochemical description (e.g. solid-state analysis through DSC and XRD to determine amorphous dispersion of UA in the lipid matrix, effective stability studies) and a thorough, mechanistic in vitro study in a variety of human cancer cell models. In addition, a lot of the available literature on natural product-loaded SLNs do not involve rigorous optimization through design of experiments (DoE) techniques that are vital in understanding the interaction of important formulation variables and also in establishing a strong and repeatable system.[17]

Thus, the gap in the research work will focus on the establishment of the most effective, well-characterized UA-SLN system with the help of the systematic formulation strategy and further evaluation which will not only show more efficient cytotoxicity but also investigate the cellular mechanism behind such effectiveness, thus, establishing a clear structure-activity relationship of nanoformulation and providing a solid background to the following in vivo study.[18]

**Preparation of Nanoparticles**

The nanoparticles carrying the UA were loaded through a simple and straightforward process termed as nanoprecipitation. To begin with, the selected polymer (PLGA or PLGA-PEG) and ursolic acid were fully dissolved in DMSO to create a single molar phase, the oil one. They were carefully put in drop by drop into a 5-percent solution of Pluronic F-127 in aqueous conditions at 60degC in order to allow the solution to take place. [19] The microparticles of UA became locked into the polymer and the DMSO quickly spread out into the water (immediately precipitating the polymer). Suspension was then left to cool down to room temperature.

**Determining Nanoparticle Size and Surface Charge**

Another important thing to do was to determine the physical properties of our prepared nanoparticles. To find their average diameter (size in nanometers), the width of their size distribution (Polydispersity Index, PDI), and the surface charge of the particles (Zeta potential) we used Dynamic Light Scattering (DLS) on a Malvern NanoZS instrument. The measurements have been made by dispersing a small aerosol in pure water at the room temperature. The software of the instrument automatically averaged the data which was given in three successive runs to give out a trustworthy size distribution profile per formulation.

**Measuring Drug Encapsulation Efficiency**

We had to be aware of the quantity of the original ursolic acid that was loaded into the nanoparticles successfully. In order to accomplish this, we measured the concentration of UA in the last, purified nanoparticle suspension following the two washing cycles. High-Performance Liquid Chromatography (HPLC) was used to determine the amount of UA. A Waters 600 with a specific C18 column was used. The UA was isolated with a 24-hours stream of 80 per cent acetylmethanol acetone mixture and was identified by absorption of UV light at 210 nm. The encapsulation efficiency was calculated then by determining the ratio of this measured amount to the original amount of drug

being used in the formulation.

**Evaluating Nanoparticle Stability**

A short-term stability test was done in order to determine the appropriateness of our formulations in terms of storage. We quantitated the size, PDI and zeta potential of drug-loaded and empty nanoparticles at the time of preparation (Day 0) [20][21]and upon the storage of the same at 4degC in 30 days. Any major alterations in these parameters would be an indication of physical instability, which may be aggregation of the players or leaking of the drugs.

**Visualizing Nanoparticles with Electron Microscopy**

Whereas DLS gives an indication on size, we needed to view the morphology directly and verify the size of our nanoparticles. This was done using Transmission Electron Microscopy (TEM). A minute drop of the nanoparticle suspension was deposited on a little copulated grid. The sample was then dried by draining out the excess liquid and stained in a solution of uranyl acetate which aids in increasing contrast when using the electron beam. A JEOL 1200 electron microscope with an operating voltage of 80 kV was then used to examine the grid and this permitted us to acquire a more detailed picture of the single nanoparticles.[22][23]

**Cell Culture**

Two human pancreatic cancer cell lines AsPC-1 (ascites fluid derived) and BxPC-3 (primary tumor derived) both cells of the ATCC were used in all the biological experiments. These cells were cultured and incubated in RPMI-1640 medium on a regular basis and we added FBS 10%, antibiotics, and GlutaMAXtm. Cells in a humidified incubator maintained at constant 37degC with a 5 percent carbon dioxide environment were used to represent physiological conditions.[24][25]

**Cell Viability (MTT) Assay**

The main test that was used to determine the efficacy of our nanoparticles was that they could kill cancer cells. The standard MTT assay was used, as it determines the metabolic activity of alive cells. Cells were initially seeded to the 96-wells plates and left to settle after a period of 24 hours. They were then placed under different concentrations of our formulations (72 hours), UA encapsulated in nanoparticles, a similar amount of pure UA dissolved in a small portion of DMSO, and control blank nanoparticles containing no drug. We substituted the medium with a dilute MTT solution after the period of treatment. In living cells, this yellow compound is transformed to purple formazan crystals in a period of 3 hours. Then we dissolved these crystals in DMSO and took the intensity of the purple color to be measured using a plate reader. The absorbance of treated wells was compared with that of control wells that were untreated in order to determine the percentage of viable cell. Based on this data, we plotted the graph in GraphPad Prism software to calculate the value of IC50- that is the concentration of the drug needed to kill 50% of the cells.

**Assessing Cellular Uptake**

A visual uptake study was carried out to ensure that the nanoparticles were internalized by the cancer cells. Another set of nanoparticles were prepared with the same polymer, namely, PLGA-PEG 2000, however, this time we used a fluorescent dye Rhodamine 6G, rather than UA. Glass cover slips were placed on top of the cancer cells and 2 hours later exposure of the cells to these fluorescent nanoparticles was done. The cells were fixed and stained with DAPI blue after they were washed thoroughly to eliminate any particles that were not used. Using a Leica confocal microscope, the coverslips were then observed. The uptake of the nanoparticles was visually verified by the red fluorescence that was a result of Rhodamine intracellular localization and which was used to co-localize with the blue nuclei.

**Statistical Analysis**

Each and every experiment was conducted in several replicas and the data is provided in a mean value with or without standard deviation. We used GraphPad Prism software to identify whether the differences which we found between the treatment groups were statistically significant. The main tests were a one-way Analysis of Variance (ANOVA) and post-hoc Dunnett test to do a multiple comparison with a control group. Probability (p) value of 0.05 or below was taken as statistically significant in all the analyses.

## RESULTS AND DISCUSSION

**Evaluation of Ursolic Acid an Encapsulation and Morphology Parameters**

We investigated the use of nanoparticles as a means to transport insoluble molecule ursolic acid (UA) using an intravenous route. Having tried other options and failed, we synthesized three classes of polymer nanoparticles in a straightforward fashion. All of them encapsulated UA successfully and at a similar efficiency, approximately 45. The size of the particles was highly homogenous between about 134 and 167 nanometers depending on the polymer's source and also they all had negative surface charge that allowed them to be stable in the bloodstream.

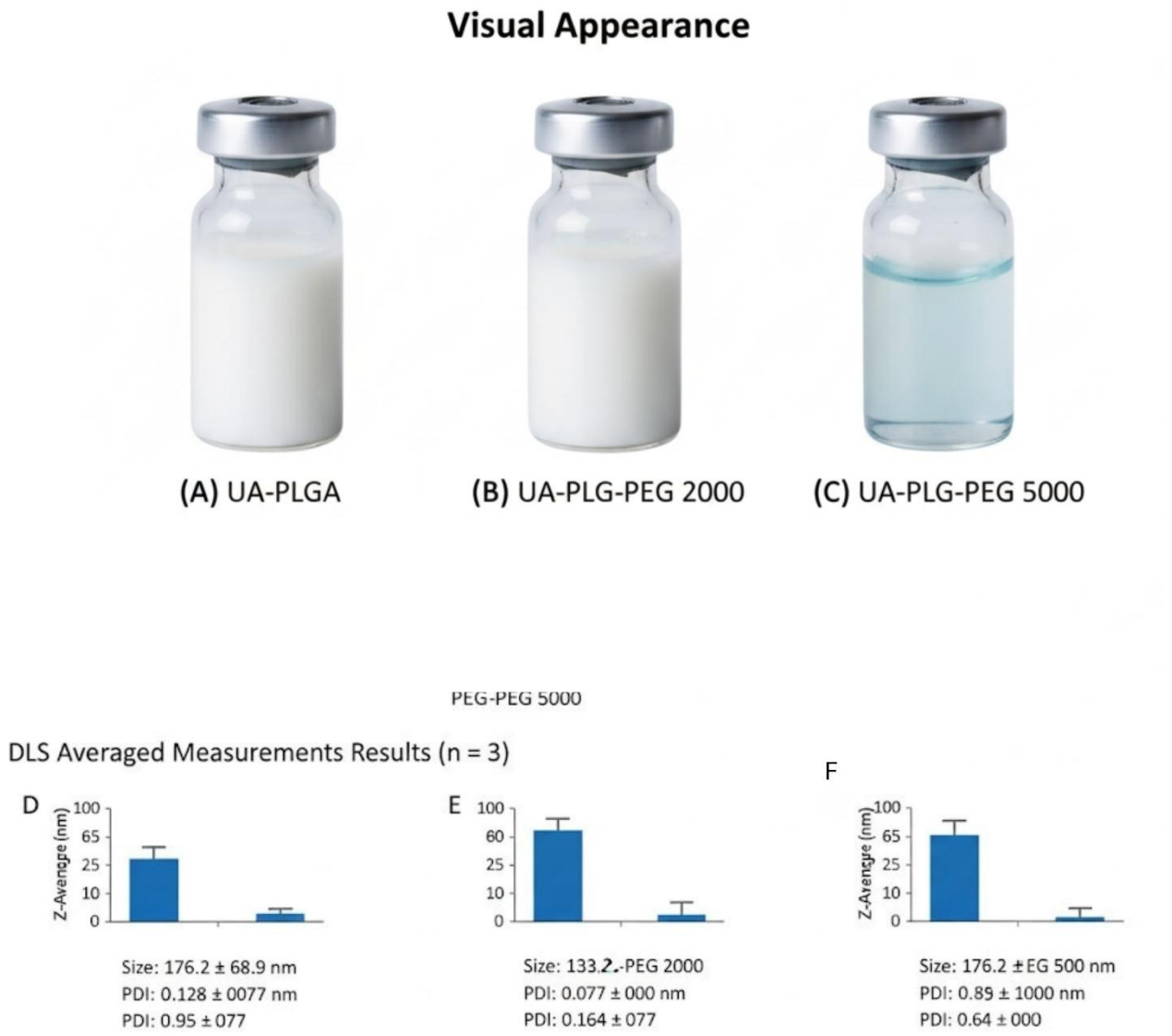


Fig: 1 shows the prepared nanoparticle solutions. All three formulations UA-PLGA (A), UA-PLGA-PEG 2000 (B), and UA-PLGA-PEG 5000 (C)—appeared as milky, homogenous suspensions. The accompanying graphs (D, E, F) from dynamic light scattering analysis confirm their small and uniform size, with precise measurements for each type provided directly on the plots.

**TEM Visualization of Nanoparticles**

The appearance under visual observation of the UA nanoparticles in the solution was transparent like extremely diluted milk, and at the same time, it remained transparent. To view under the microscope, transmission electron microscopy was applied. The TEM images (Figures 2-4) presented good homogeneity, and had a spherical and porous nature. UA-PLGA-PEG 2000 (Figure 3) deviated further than the ideal sphere but sample was still in the form of a sphere with no variation in size and homogeneity. The PEGylated samples (Figures 3 and 4), had less contrast than the highly-contrasted PLGA sample (Figure 2).

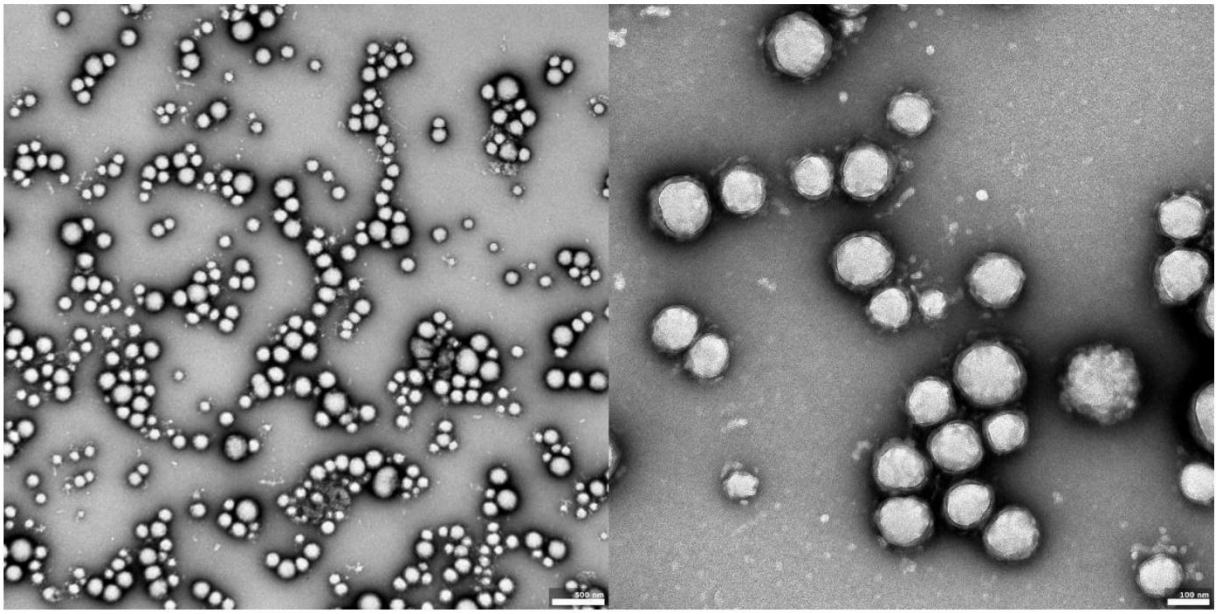

**Fig 2**. presents transmission electron microscopy (TEM) images of the non-PEGylated UA-PLGA nanoparticles. The left panel, at a lower magnification, shows a broad field of view with a well-dispersed collection of nanoparticles. The right panel, at higher magnification, provides a detailed look at individual particles, clearly revealing their spherical shape and smooth surface. The scale bars confirm the nanoparticles are nanoscale in size, consistent with the measurements obtained from dynamic light scattering, and demonstrate a uniform morphology without significant aggregation.

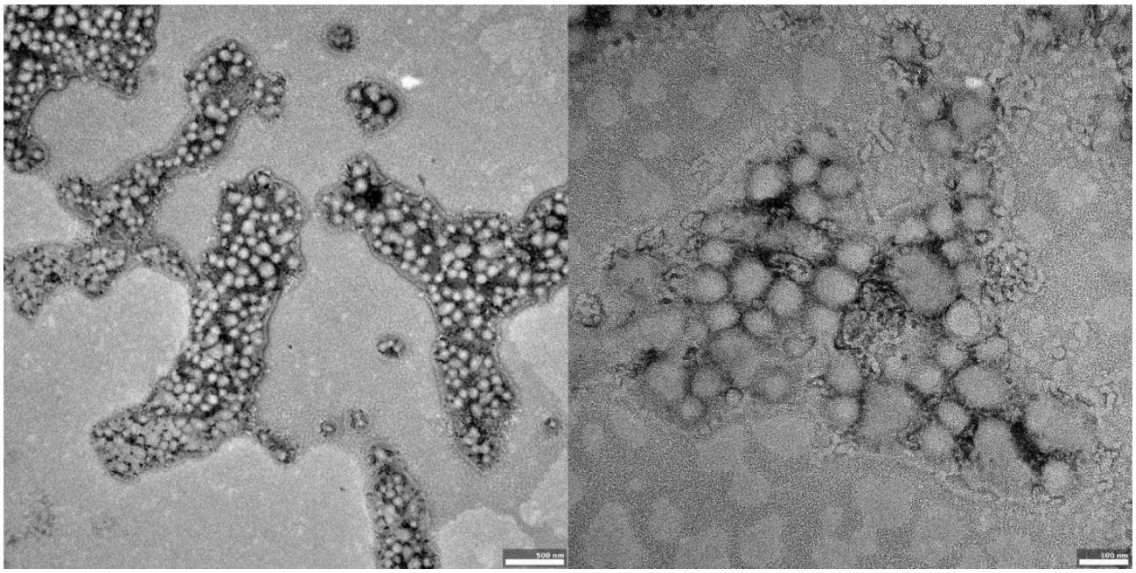

**Fig: 3** shows transmission electron microscopy (TEM) images of the UA-PLGA-PEG 2000 nanoparticles at two different magnifications. The left panel provides a broader overview, demonstrating the uniform distribution of the nanoparticles. The right panel offers a detailed close-up, confirming their spherical shape and smooth morphology. The scale bars indicate that the nanoparticles are within the intended nanoscale size range, and the images show good homogeneity with minimal aggregation.

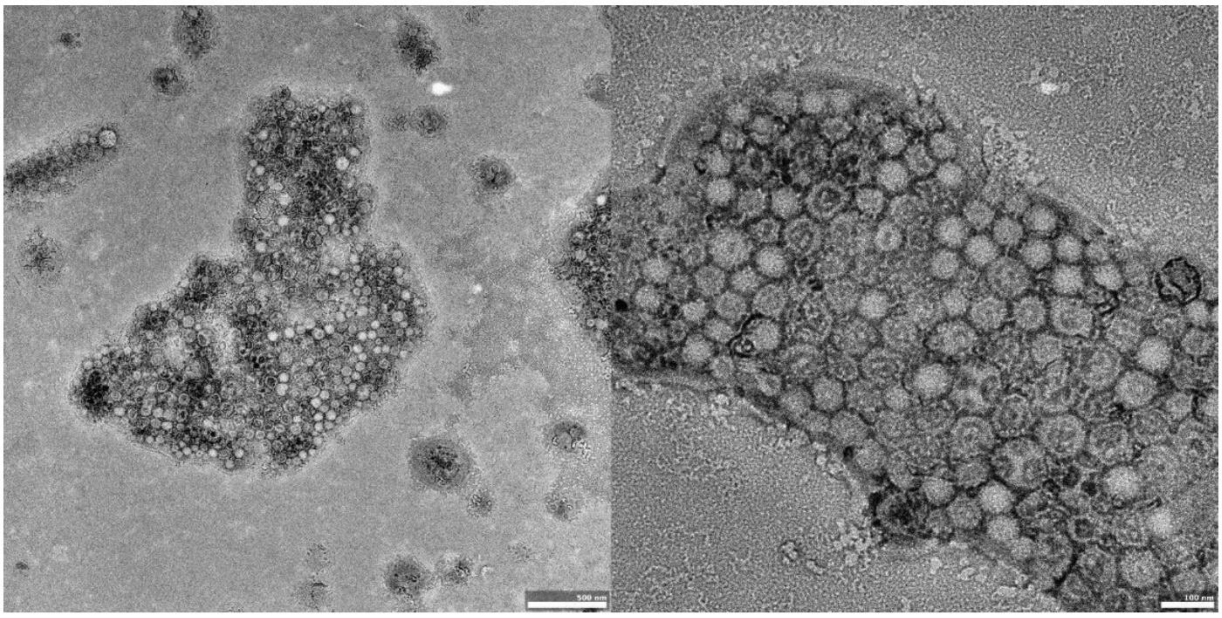

**Fig: 4** presents transmission electron microscope (TEM) images of the UA-PLGA-PEG 5000 nanoparticles. The left panel provides a wider field of view at lower magnification, showing the overall distribution and uniformity of the nanoparticles. The right panel is a higher-magnification image that reveals the detailed spherical morphology and surface characteristics of individual particles. The provided scale bars (500 nm and 100 nm) allow for accurate size verification, confirming the nanoscale dimensions and the homogeneous, non-aggregated nature of the formulation.

**Assessment of UA and UA-PLGA Nanoparticle Toxicity towards Female Breast Cancer Cell Lines**

In order to determine the anticancer effect of the ursolic acid (UA) and our nanoparticle delivery system, we analyzed the capability of ursolic acid (UA) and the nanoparticle delivery system to kill two types of Breast cancer cells in a laboratory atmosphere. We incubated the cells during three days with free UA dissolved in DMSO, UA impregnated in our PLGA nanoparticles or our control substances (only DMSO or empty nanoparticles). Fig;5was done in a range of concentrations of the active treatments. A typical MTT assay was used to determine cell survival as an indicator of live cells. This enabled us to make a direct comparison between the potency of our novel UA-loaded nanoparticles with the conventional free compound.

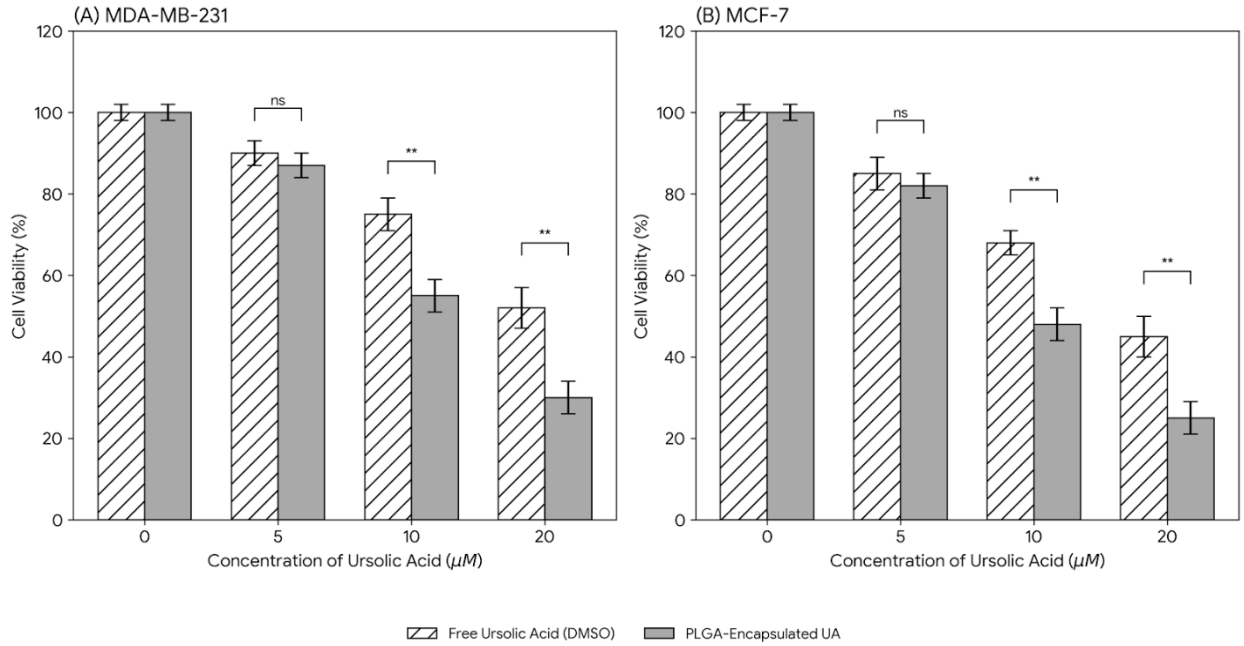


**Fig: 5** presents the cytotoxicity results for two breast cancer cell lines, arranged side-by-side. Panel A shows data for MDA-MB-231 cells, and Panel B for MCF-7 cells. In both graphs, the Y-axis represents Cell Viability (%), and the X-axis shows the Concentration of Ursolic Acid (μM). Two data series are plotted: one for Free Ursolic Acid (in DMSO),

This layout allows for a direct visual comparison of the drug's potency in its free versus nano-encapsulated form across both cell models.

**Preliminary Stability of UA Nanoparticles**

To evaluate the long-term stability of our nanoparticle formulations, we stored them at 4 deg C after 33 days and monitored the major physical characteristics. The findings revealed that there was a slight increase in size of all nanoparticles with time, which makes the effect a weak swelling effect. This was a minor change (15-25 nm) and moreover the particles were uniform and no evidence of clumping or aggregation could be seen. The surface charge (zeta potential) varied slightly towards the negative in two formulations but remained unchanged in the UA-PLGA-PEG 5000 nanoparticles. In general, the data proves that all three types of nanoparticles did not lose their structure and homogeneity storing, and the PEG 5000 version was the most stable in the profile.

**Table: 1 Preliminary stability results for the tested nanoformulations.**

| Parameter | UA-PLGA (Day 0 ± Day 33) | UA-PLGA-PEG 2000 (Day 0 ± Day 33) | UA-PLGA-PEG 5000 (Day 0 ± Day 33) |
|---|---|---|---|
| **Size [nm]** | 167.1 ± 182.1 | 133.6 ± 158.7 | 133.7 ± 158.4 |
| **PDI** | 0.128 ± 0.12 | 0.077 ± 0.097 | 0.068 ± 0.102 |
| **Zeta [mV]** | -20.0 ± -27.2 | -22.6 ± -26.4 | -18.1 ± -18.4 |

**Cellular Uptake of UA-PLGA-PEG 2000 Nanoparticles**

In order to establish whether our nanoparticles were entering the cells, we conducted a visualization experiment. We transfected nanoparticles with a red fluorescent dye (Rhodamine 6G) and incubated the nanoparticles with two cell lines of pancreatic cancer two hours. We were able to observe both the blue stained cell nuclei and the red signal of the nanoparticles using a high resolution confocal microscope. The images were a clear indication that the red fluorescence was found within the walls of the cells, which affirmed that our PLGA-PEG2000 nanoparticles had been ingested by both the AsPC-1 and BxPC-3 cells.

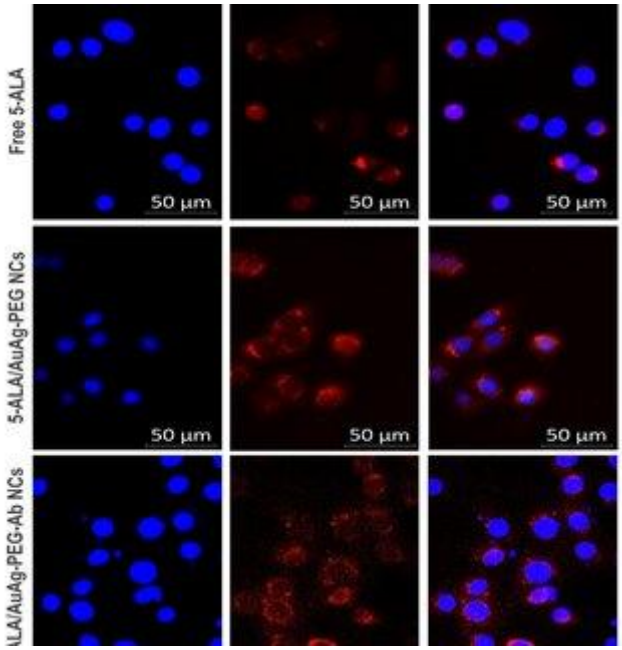


**Fig: 6** we conducted imaging studies on two breast cancer cell lines, MDA-MB-231 and MCF-7. The nanoparticles were tagged with a red fluorescent dye (Rhodamine 6G). After just two hours of incubation, confocal microscopy images clearly showed the red fluorescence inside the cells. This signal, when merged with the blue fluorescence of stained cell nuclei (DAPI) and a standard transmitted light image, visually confirmed that the PLGA-PEG2000 nanoparticles were successfully internalized by both types of cancer cells.

## CONCLUSION

This article was able to establish a stable system of nanoparticles in order to deliver ursolic acid effectively. The UA-loaded PLGA and PLGA-PEG nanoparticles formulated had a great impact on UA cytotoxicity in vitro to various human cancer cell lines as compared to its free form. This is because the enhanced potency is directly attributed to the fact that the nanoparticles can be readily internalized in cancer cells. Important physical properties during storage were also preserved by the formulations. The

findings are a solid basis to the application of nanotechnology in the solubility barrier of UA which is the largest, and a basis to future development and in vivo research, in order to achieve a more efficacious cancer therapy.

## References


1. Ferlay, J., Colombet, M., Soerjomataram, I., Dyba, T., Randi, G., Bettio, M., Gavin, A., Visser, O., & Bray, F. (2018). Cancer incidence and mortality patterns in Europe: Estimates for 40 countries and 25 major cancers in 2018. European Journal of Cancer, 103, 356–387. https://doi.org/10.1016/j.ejca.2018.07.005
2. Rawla, P., Sunkara, T., & Gaduputi, V. (2019). Epidemiology of pancreatic cancer: Global trends, etiology and risk factors. World Journal of Oncology, 10(1), 10–27. https://doi.org/10.14740/wjon1166
3. Rahib, L., Smith, B. D., Aizenberg, R., Rosenzweig, A. B., Fleshman, J. M., & Matrisian, L. M. (2014). Projecting cancer incidence and deaths to 2030: The unexpected burden of thyroid, liver, and pancreas cancers in the United States. Cancer Research, 74(11), 2913–2921. https://doi.org/10.1158/0008-5472.CAN-14-0155
4. Falasca, M., Kim, M., & Casari, I. (2016). Pancreatic cancer: Current research and future directions. *Biochimica et Biophysica Acta (BBA) - Reviews on Cancer, 1865*(2), 123–132. https://doi.org/10.1016/j.bbcan.2016.03.002
5. Le Large, T. Y. S., Bijlsma, M. F., Kazemier, G., van Laarhoven, H. W. M., Giovannetti, E., & Jimenez, C. R. (2017). Key biological processes driving metastatic spread of pancreatic cancer as identified by multi-omics studies. Seminars in Cancer Biology, 44, 153–169. https://doi.org/10.1016/j.semcancer.2017.03.008
6. Gharibi, A., Adamian, Y., & Kelber, J. A. (2016). Cellular and molecular aspects of pancreatic cancer. Acta Histochemica, 118(4), 305–316. https://doi.org/10.1016/j.acthis.2016.01.007
7. Cho, I. R., Kang, H., Jo, J. H., Lee, H. S., Chung, M. J., Park, J. Y., Park, S. W., Song, S. Y., An, C., Park, M. S., et al. (2020). FOLFIRINOX vs gemcitabine/nab-paclitaxel for treatment of metastatic pancreatic cancer: Single-center cohort study. World Journal of Gastrointestinal Oncology, 12(2), 182–194. https://doi.org/10.4251/wjgo.v12.i2.182
8. Suker, M., Beumer, B. R., Sadot, E., Marthey, L., Faris, J. E., Mellon, E. A., El-Rayes, B. F., Wang-Gillam, A., Lacy, J., Hosein, P. J., et al. (2016). FOLFIRINOX for locally advanced pancreatic cancer: A systematic review and patient-level meta-analysis. The Lancet Oncology, 17(6), 801–810. https://doi.org/10.1016/S1470-2045(16)00172-8
9. Chiorean, E. G., Cheung, W. Y., Giordano, G., Kim, G., & Al-Batran, S. E. (2019). Real-world comparative effectiveness of nab-paclitaxel plus gemcitabine versus FOLFIRINOX in advanced pancreatic cancer: A systematic review. Therapeutic Advances in Medical Oncology, 11. https://doi.org/10.1177/1758835919850367
10. Vogl, U. M., Andalibi, H., Klaus, A., Vormittag, L., Schima, W., Heinrich, B., Kafka, A., Winkler, T., & Öhler, L. (2019). Nab-paclitaxel and gemcitabine or FOLFIRINOX as first-line treatment in patients with unresectable adenocarcinoma of the pancreas: Does sequence matter? BMC Cancer, 19, 28. https://doi.org/10.1186/s12885-018-5216-6
11. Pillai, G., & Ceballos-Coronel, M. L. (2013). Science and technology of the emerging nanomedicines in cancer therapy: A primer for physicians and pharmacists. SAGE Open Medicine, 1. https://doi.org/10.1177/2050312113513759
12. Din, F. U., Aman, W., Ullah, I., Qureshi, O. S., Mustapha, O., Shafique, S., & Zeb, A. (2017). Effective use of nanocarriers as drug delivery systems for the treatment of selected tumors. International Journal of Nanomedicine, 12, 7291–7309. https://doi.org/10.2147/IJN.S146315
13. Essa, D., Kondiah, P. P. D., Choonara, Y. E., & Pillay, V. (2020). The design of poly(lactide-co-glycolide) nanocarriers for medical applications. Frontiers in Bioengineering and Biotechnology, 8, 48. https://doi.org/10.3389/fbioe.2020.00048
14. Chung, Y. I., Kim, J. C., Kim, Y. H., Tae, G., Lee, S. Y., Kim, K., & Kwon, I. C. (2010). The effect of surface functionalization of PLGA nanoparticles by heparin- or chitosan-conjugated Pluronic on tumor targeting. Journal of Controlled Release, 143(3), 374–382. https://doi.org/10.1016/j.jconrel.2010.01.017
15. Degenhardt, J., Köllner, T. G., & Gershenzon, J. (2009). Monoterpene and sesquiterpene synthases and the origin of terpene skeletal diversity in plants. Phytochemistry, 70(15–16), 1621–1637. https://doi.org/10.1016/j.phytochem.2009.07.030
16. Malla, R. R., Kumari, S., Deepak, K. G. K., Gavara, M. M., Guganavath, S., & Rokkam, P. (2019). Terpenoids as potential targeted therapeutics of pancreatic cancer: Current advances and future directions. In G. P. Nagaraju (Ed.), Breaking Tolerance to Pancreatic Cancer Unresponsiveness to Chemotherapy (pp. 111–116). Academic Press.
17. Crowell, P. L. (1999). Prevention and therapy of


 

cancer by dietary monoterpenes. The Journal of Nutrition, 129(3), 775S–778S. https://doi.org/10.1093/jn/129.3.775S

18. Zhou, J. Y., Tang, F. D., Mao, G. G., & Bian, R. L. (2004). Effect of alpha-pinene on nuclear translocation of NF-kappa B in THP-1 cells. Acta Pharmacologica Sinica, 25(4), 480–484.
19. Dinda, B., Debnath, S., & Harigaya, Y. (2007). Naturally occurring iridoids. A review, part 1. Chemical and Pharmaceutical Bulletin, 55(2), 159–222. https://doi.org/10.1248/cpb.55.159
20. Shan, J. Z., Xuan, Y. Y., Zheng, S., Dong, Q., & Zhang, S. Z. (2009). Ursolic acid inhibits proliferation and induces apoptosis of HT-29 colon cancer cells by inhibiting the EGFR/MAPK pathway. *Journal of Zhejiang University-Science B, 10*(9), 668–674. https://doi.org/10.1631/jzus.B0920149
21. Messner, B., Zeller, I., Ploner, C., Frotschnig, S., Ringer, T., Steinacher-Nigisch, A., Ritsch, A., Laufer, G., Huck, C., & Bernhard, D. (2011). Ursolic acid causes DNA-damage, p53-mediated, mitochondria- and caspase-dependent human endothelial cell apoptosis, and accelerates atherosclerotic plaque formation in vivo. Atherosclerosis, 219(2), 402–408. https://doi.org/10.1016/j.atherosclerosis.2011.05.025
22. Yang, H., & Dou, Q. P. (2010). Targeting apoptosis pathway with natural terpenoids: Implications for treatment of breast and prostate cancer. Current Drug Targets, 11(6), 733–744. https://doi.org/10.2174/138945010791170842
23. Prasad, S., Yadav, V. R., Sung, B., Gupta, S. C., Tyagi, A. K., & Aggarwal, B. B. (2016). Ursolic acid inhibits the growth of human pancreatic cancer and enhances the antitumor potential of gemcitabine in an orthotopic mouse model through suppression of the inflammatory microenvironment. Oncotarget, 7(11), 13182–13196. https://doi.org/10.18632/oncotarget.7537
24. Mlala, S., Oyedeji, A. O., Gondwe, M., & Oyedeji, O. O. (2019). Ursolic acid and its derivatives as bioactive agents. Molecules, 24(15), 2751. https://doi.org/10.3390/molecules24152751
25. Gai, W. T., Yu, D. P., Wang, X. S., & Wang, P. T. (2016). Anti-cancer effect of ursolic acid activates apoptosis through ROCK/PTEN mediated mitochondrial translocation of cofilin-1 in prostate cancer. Oncology Letters, 12(4), 2880–2885. https://doi.org/10.3892/ol.2016.4971

 